Journal of Magnetics 7(2), 45-50 (2002)

A Study of Magnetic Field Annealing on Microstructures and Magnetic Properties of Nanocomposite Sm-Co/Co Films

Choong Jin Yang*, Cai Yin You[1,2], Z. D. Zhang[1], Kyung Soo Kim[2] and Jong Soo Han[2]

[1]*Institute of Metal Research, Academia Sinica,Shenyang 110016, Peoples Republic of China*
[2]*Electromagnetic Materials Laboratory, Research Institute of Industrial Science and Technology (RIST), P.O. Box 135, Pohang 790-330, Korea*

(Received 21 May 2002)

A magnetic field annealing is firstly used for nanostructured Sm-Co/Co films, prepared by magnetron sputtering method. The effects of magnetic field annealing on single-layered Sm-Co films are different from those on multi-layered Sm-Co/Co films. A detailed analysis of microstructures and magnetic properties is made by means of HRTEM, Auger electron spectroscopy, XRD and Physical Property Measurement System (PPMS). From magnetic properties and microstructure analysis, it was confirmed that these differences originate from the effects of magnetic field annealing on crystallization behavior of the films. The relationship between magnetic properties and microstructures explains a different demagnetization process of single-layered and multi-layered films. For the single-layered Sm-Co films, magnetic-field-annealing makes the main phases change from $CaCu_5$ to Zn_2Th_{17} structure, resulting in a decrease of coercivity. The results show that the magnetic-field-annealing is useful to improve the properties of nanostructured Sm-Co(30 nm)/Co(10 nm) films, which ascribe to improving the pinning effectiveness in coercivity mechanism and decreasing the magnetostatic interaction of films. A very high coercivity about 0.7 T was obtained from nanoscaled multi-layered Sm-Co(30 nm)-/Co(10 nm) films.

Key words : Multilayers, Magnetic field annealing, Auger electron spectra, Coercivity

1. Introduction

Sm-Co thin films are widely studied due to potential application for high-density hard disk magnetic recording media and for a use of micro devices. F.J. Cadieu group widely investigates the synthesis, and anisotropy of Sm-Co based films [1-3]. E.M. Velu group widely investigates the microstructure and effects on longitudinal recording [4,5]. Eric E. Fullerton *et al.* widely study the microstructures and properties of the epitaxial rare-earth-transition-metal films [6, 7]. Some authors also investigate microstructure of Cr underlayer and its effects [8, 9].

Now nanocomposite films are very attractive due to many merits such as remanence enhancement, high magnetic energy product. Eric E. Fullerton *et al.* study the structure and magnetic properties of epitaxial Sm-Co/Co superlattices prepared by magnetron sputtering [10]. J.P. Liu *et al.* and R. Andreescu *et al.* study the magnetic hardening in $SmCo_x$-Co multilayers [11, 12].

In this study magnetic-heat-treatment is firstly used for nanostructured Sm-Co/Co films during the crystallization of film structure. A different effect of magnetic-heat-treatment is observed for single layer of hard magnetic films and nanocomposite films. It can be understood from the relationship between microstructures and magnetic properties.

2. Experimental Procedure

Three kinds of Sm-Co/Co films with Ta underlayer and toplayer,

substrate(Si)/Ta(60 nm)/Sm-Co(200 nm)/Ta(60 nm);
substrate(Si)/Ta(60 nm)/[Sm-Co(30 nm)/Co(6 nm)]^{10}/Ta(60 nm);
substrate(Si)/Ta(60 nm)/[Sm-Co(30 nm)/Co(10 nm)]^{10}/Ta(60 nm).

were prepared with a multiple-gun rf-sputtering system by sputtering the target onto silicon substrate. The $SmCo_5$

*Corresponding author: Tel: +82-54-279-6331, e-mail: cjyang@rist.re.kr

target was made by compressing the powders of $SmCo_5$ alloy, and by sintering at 1000°C. Ta and Co targets were made by alloying the pure elements (>99.9 wt.%). Flowing high-purity argon gas at 10 mTorr was used and base pressure of sputtering system is lower than 2×10^{-6} Torr. The as-deposited films were then annealed in a furnace at a vacuum 5×10^{-6} Torr under a 4.5 kG field along in-plane direction or without field.

Magnetization loops were measured by a vibrating sample magnetometer (VSM), an alternating gradient magnetometer (AGM) and physical property measurement system (PPMS). Phase ingredient and compositions were identified by XRD and auger electron spectra. The thickness of films was measured by using α-step (Tencor Instrument, Inc.) and calculated by Auger electron spectra. The microstructures were observed by a transmission electron microscopy.

3. Results and Discussion

Fig. 1 shows the XRD patterns of Sm-Co single-layered films and [Sm-Co(30 nm)/Co(10 nm)]^{10} nanocomposite films, which are as-deposited and as-annealed at 630 °C. The as-deposited films were confirmed to be amorphous with some $SmCo_5$ crystals of (301) orientation. All films

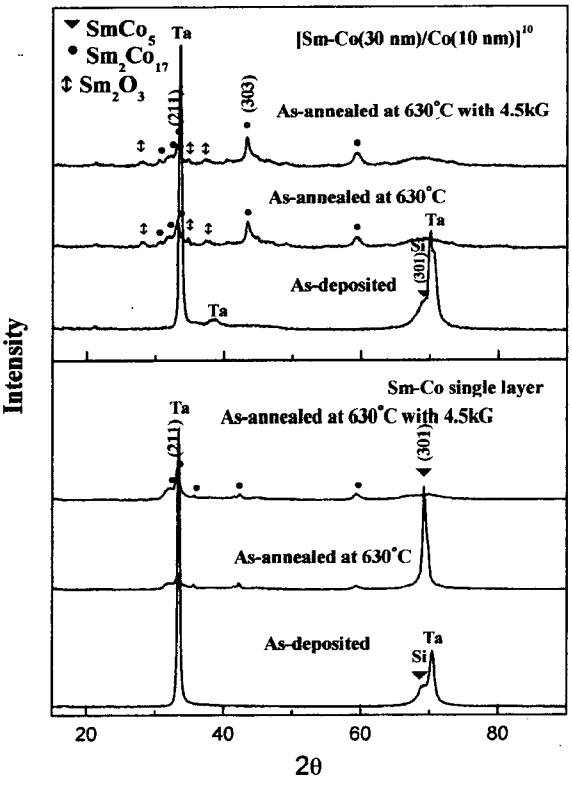

Fig. 1. The XRD patterns of Sm-Co single-layered films and [Sm-Co(30 nm)/Co(10 nm)]^{10} multi-layered films.

had obviously weak preferred orientation. For the single-layered, the main phase was $SmCo_5$ of (301) preferred orientation with a trace of Sm_2Co_{17} phase after annealed at 630 °C. For [Sm-Co(30 nm)/Co(10 nm)]^{10} nanocomposite films, the main phase was Sm_2Co_{17} phase with a trace of $SmCo_5$ phase after annealed at 630 °C. Sm_2Co_{17} phase shows a weak (211) preferred orientation because the diffraction (211) is very weak for a random polycrystals. Cadieu group reported that preferred orientation of micro-thickness films changes from (110) to (200) with decreasing oxygen level or increasing the deposition rate and lowering the film deposition pressure [1-3]. The films with (110) preferred orientation have higher coercivities [3]. Fullerton *et al.* reported that all Sm-Co and Co layers have the same easy-axis direction due to structural coherence for epitaxial Sm-Co/Co superlattices [10]. The structure of the superlattices is twinned due to the two-fold Sm-Co $(11\bar{2}0)$ growth alignment with respect to the four-fold symmetry of the Cr(100) buffer layer. The two epitaxial relations are Sm-Co[0001] || Cr[011] || MgO[010] and Sm-Co[0001] || Cr[011] || MgO[001]||. All the reflections indicate that the magnetic easy axis lie in the film plane. Our preferred orientation is different from theirs because of different process. Above films are all deposited at pre-heated substrate and have no post deposition heat treatment. For our weak films orientation is obtained by annealing the as-deposited films.

Magnetic heat treatment is widely used for bulk magnetic material. It has been learned to be useful for a grain refinement and uniformity. In this study we firstly introduce this technique to multi-layered nanocomposite films. The effects of magnetic heat treatment for the nanoscaled films were different from those for bulk materials. Applying a field at 4.5 kG in film plane during annealing, the main phase changes from $CaCu_5$ structure to Th_2Zn_{17} structure in a weak preferred (211) orientation for the single-layered films. For multi-layered nanocomposite films, however, annealing the films at 630 °C at a 4.5 kG magnetic field makes the main diffraction peak of Th_2Zn_{17} (303) intensive. The intensity ratio of (211) peak to (303) peak changes from 1.05 to 0.8 compared with 0.05 in JCPDS standard card. This means that applying field promotes the crystallization of films.

Fig. 2 (a, b, c, and d) shows the TEM images of the samples studied. The figure (a) is of Sm-Co single-layer after annealing at 630 °C at 4.5 kG. The figure (b) is of the as-deposited nanocomposite [Sm-Co(30 nm)/Co(10 nm)]^{10} film. The figured (c) is of the sample (b) after annealing at 630 °C at 4.5 kG, and the figure (d) is the selected area HRTEM for the image (c). For the single-layered films, the magnetic layer is composed of nano-

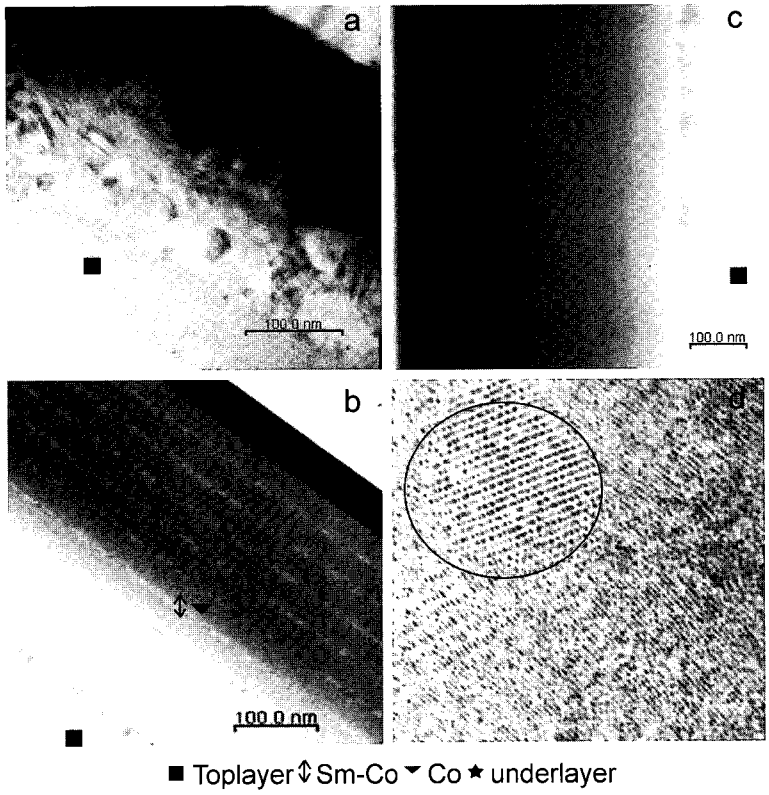

Fig. 2. The TEM images of the samples of single-layered and multi-layered films (Co=10 nm).

scaled crystallites all over the layer as shown in Fig. 2(a). From Fig. 2(b), the ten-layered structure is clearly shown after deposition. But after annealing the nanocomposite films, it is hard to distinguish each magnetic layer and crystals. Because the thickness of Sm-Co and Co layer is about 30 nm and 10 nm, respectively, the crystallites of each hard and soft magnetic layers became nano-sized particles after annealing. Fig. 2(d) shows a HRTEM image of a crystal marked by circle, which indicates a nano-crystal smaller than 10 nm.

Fig. 3 shows the compositional change of films profile by using Auger electron spectra. It was firstly confirmed that a refined auger electron spectroscopy could also give detailed information of multi-layered films. It is clearly shown that the compositional changes along the depth of films are dominant due to the compositional gradient existing at the interface of layers. It can be seen that annealing process changes the distribution of elements along the depth of films. The annealing process introduces some oxygen that interacts with corresponding Sm element preferentially, which is obviously shown by the depth profile of O element. Co element, however, is free from oxidation. The Ta and Co elements are preferential to inter-diffuse each other. The Ta elements reject the diffusion of Sm elements. This is consistent with the phase diagrams of Ta-Co and Ta-Sm [13]. So the inter-diffusion of Ta and Co affects the diffusion of Sm element. Due to the binding of Sm to Co the inter-diffusion is mainly the diffusion of Ta into Co. When applying a magnetic field along the plane of films during annealing, the depths of elements were enlarged compared with without magnetic field. It suggests that the applied field dominantly activates the diffusion of Co to alloy hard magnetic phase, Sm_2Co_{17}. Consequently it promotes the inter-diffusion of elements in the matrix of thin films. From the results of Auger electron spectra, the diffusion of Si to the magnetic films can be avoided by using a Ta underlayer. One can realize that each peak of Sm profile corresponds to each valley of Co profile.

For the films of Sm-Co single-layer, magnetic properties decrease with applying the magnetic field during annealing. Applying magnetic field at 600 °C, coercivity decreases from 46 kOe to 41 kOe. For the sample annealed at 630 °C with a magnetic field, the coercivity about 39 kOe is lower than that at 600 °C. This is consistent with the fact that the main phase changes from $CaCu_5$ structure to Th_2Zn_{17} structure. (cf. Fig. 1) Also for the [Sm-Co(30 nm)/Co(6 nm)]^{10} nanocomposite films by applying the magnetic field during annealing in our study causes the coercivity to decrease from 47 kOe to 45 kOe

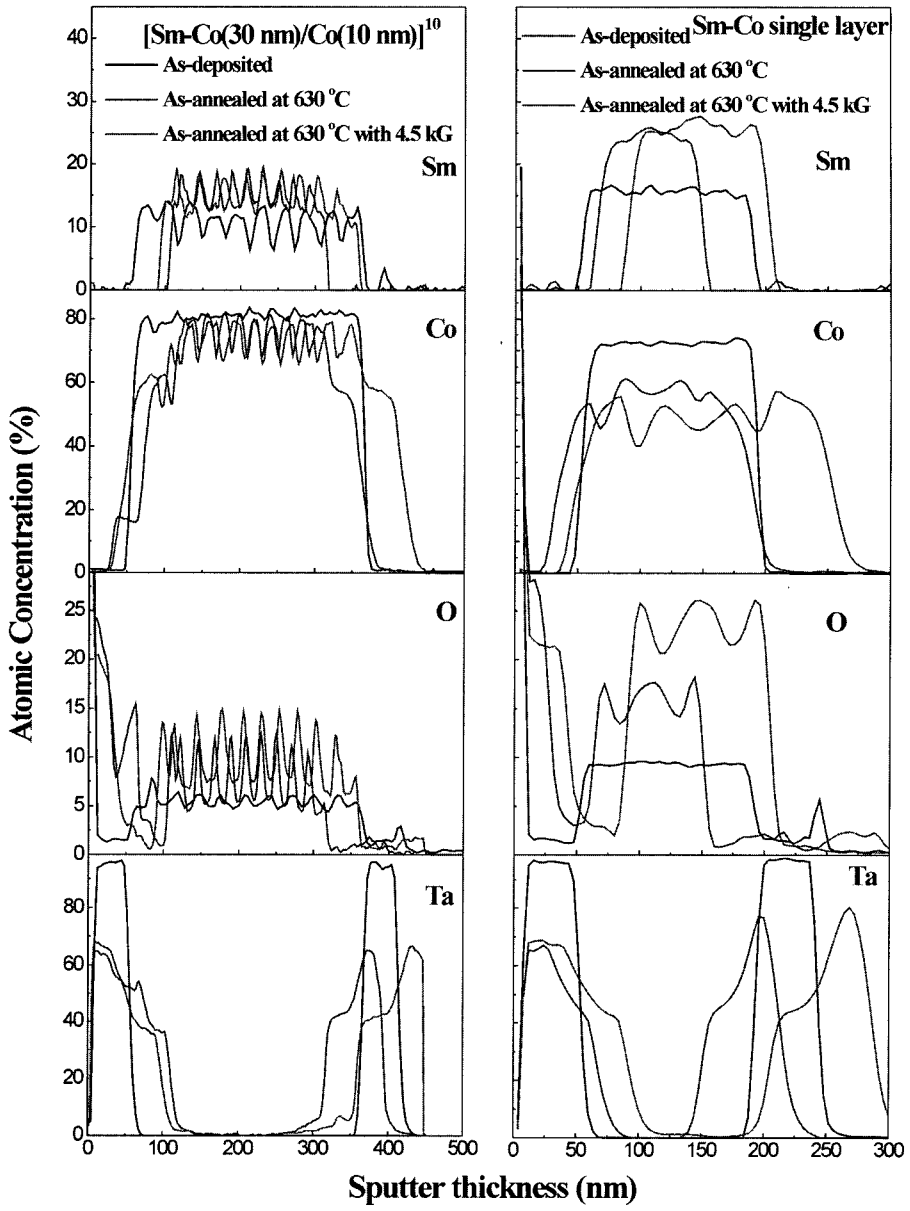

Fig. 3. The compositional depth profile of single-layered and multi-layered (Co=10 nm) by using Auger electron spectra.

at 630 °C heat treatment, from 26 kOe to 19 kOe at 600 °C heat treatment, respectively. This data is not shown in this paper but the obtained magnetic properties were almost times higher than those of multilayered films of [Sm-Co(30 nm)/Co(10 nm)]^{10} [16]. Liu *et al.* and R. Andreescu *et al.* also reported an approximate coercivity for multilayers [11, 12].

For the nanocomposite films with a thick soft Co layer (10 nm), however, applying the magnetic field during annealing increases the coercivity. The films seem not to exhibit the plane anisotropy because the magnetic hysteresis loops along parallel direction to film plane are similar to that along perpendicular direction to film plane. It is in agreement with the results of XRD, showing a preferred (211) orientation in the plane and the easy magnetization axis of $SmCo_5$ and/or Sm_2Co_{17} crystals does not exist within the plane. Fig. 4 shows the magnetic hysteresis loops for the multi-layered films (Co thickness 10 nm), $m_r(H)$, and $m_d(H)$ plots are also made. The isothermal remanence $m_r(H)$ ($M_r(H)/M_r(\infty)$) was measured by a progressive magnetization of an initially ac-demagnetized sample, and $m_d(H)$ ($M_d(H)/M_r(\infty)$) was measured by a progressive demagnetized from a previously saturated state [14]. Applying the magnetic field during

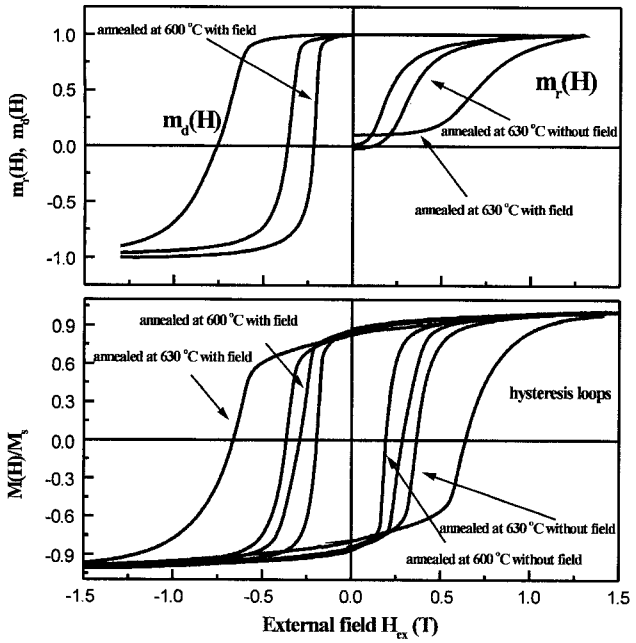

Fig. 4. The magnetic hysteresis loops, $m_r(H)$, and $m_d(H)$ plots for the multi-layered films [Sm-Co(30 nm)/Co(10 nm)]^{10}.

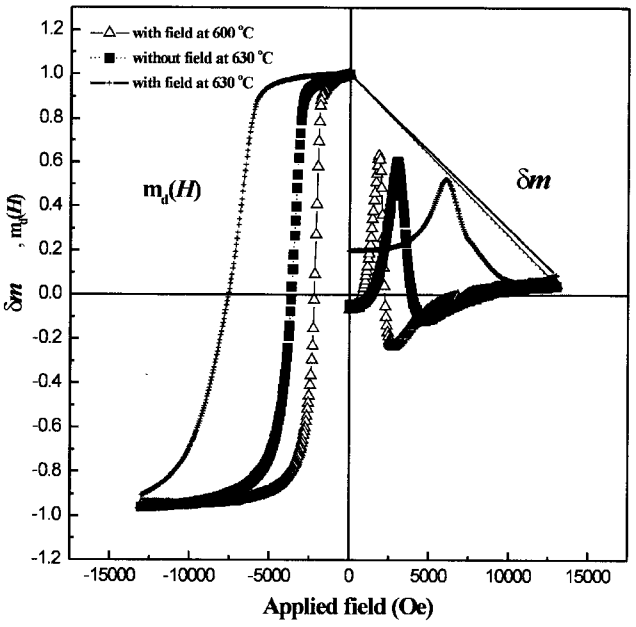

Fig. 5. Variation of the Demagnetization remanence $m_d(H)$, δm with the external magnetic field of [Sm-Co(30 nm)/Co(10 nm)]^{10} multi-layered films.

heat treatment, especially for those annealed at 630 °C, the enhancement of coercivity is obvious. For $m_d(H)$ plot, when the applied field is lower than the coercive force of films, the demagnetization remanence $m_d(H)$ hardly decreases, indicating a reversible region of demagnetization process. This is the typical behavior for the exchange-

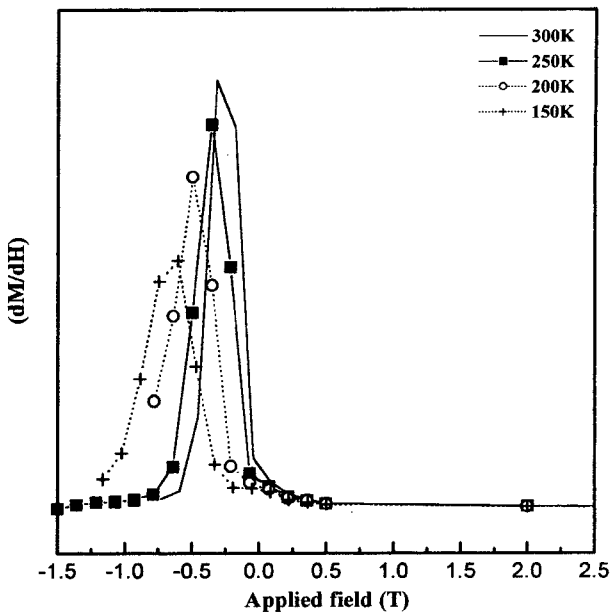

Fig. 6. The SFD (switch field distribution) curve of the sample [Sm-Co(30 nm)/Co(10 nm)]^{10} annealed at 630 °C at 4.5 kG.

spring magnets. Obviously, the $m_r(H)$ curve of the sample annealed at 630 °C with 4.5 kG field is very different from others. It seems to represent a different coercivity mechanism supposing an improved pinning effectiveness.

The parameter δm, $\delta m = m_d(H)-(1-2m_r(H))$, is a direct measure of the magnetic interactions between the soft and hard magnetic phases [14]. In order to obtain some insight into the magnetic interactions, we examine the δm curves (shown in Fig. 5) obtained by using AGM. Positive values of dm are due to the exchange coupling promoting the magnetized state, whereas negative values are due to the magnetostatic interactions tending to assist the magnetization reversal of the grains. Prados and Hadjipanayis [15] reported a similar nature and magnitude magnetizing interaction (δm is always positive) for Sm(Co, Cu, Ni) thin films, which show a quite different coercivity. It was supposed that the increase of the annealing temperature improves the pinning effectiveness with the high frequency of crystallites reaching the optimum level [11]. It is also reasonable for us to suppose that applying the magnetic field during the heat treatment has the effect similar to that of increasing the annealing temperature, because of the activation of the diffusion process being confirmed by the depth profile of the films by Auger electron spectra. Moreover, from the values of δm, it is concluded that the magnetic field heat treatment could decrease the magnetostatic interaction due to more uniform structure, so increase the coercivity (cf. Fig. 4).

In order to confirm further the exchange interaction, the

SFD (switch field distribution) at different measurement temperature for the sample (Co thickness 10 nm) annealed at 630 °C with a magnetic field is shown in Fig. 6. The peak decreases and widens with decreasing measurement temperature. It means that exchange interaction weakens with decreasing the measurement temperature due to magnetic hardening. This is the feature of exchange coupling, where exchange-coupling length ($\pi A_{eff}/K_{eff}$) decreases due to magnetic hardening with decreasing environmental temperature.

4. Conclusions

Applying a magnetic field during annealing makes the main phases change from $CaCu_5$ to Th_2Zn_{17} structure for a single-layered films, resulting in a decrease of coercivity. It was confirmed that a refined Auger electron spectroscopy could also give detailed information of compositional profile of magnetic interfaces. Applying the magnetic field during annealing increases the coercivity of nanocomposite films with a thick soft Co layer (10 nm). It is mainly ascribed to the increase of pinning effectiveness in the nanoscaled magnetic hard phase. However, exchange interaction becomes weaker with decreasing the environmental temperature.

Acknowledgements

This work was financially supported by The Korean Ministry of Science & Technology under Project Contract No. 2001D711 ("National Core Project on nanoscaled Materials", KIST), and also supported by The research Center for Advanced Magnetic Material (Choongnam National Univ.) under Contract No.2001D008.

References

[1] F. J. Cadieu, T. D. Cheung, S. H. Aly, and L. Wickramasekara, R. G. Ririch, J. Appl. Phys. **53**, 8338 (1982).
[2] H. Hegde, P. Samarasekara, R. Rani, A. Navarathna, K. Tracy, and F. J. Cadieu, J. Appl. Phys. **76**, 6760 (1994).
[3] R. Rani, F. J. Cadieu, X. R. Qian, W. A. Mendoza, and S. A. Shaheen, J. Appl. Phys. **81**, 5634 (1997).
[4] E. M. T. Velu, and D. N. Lambeth, IEEE Trans. Magn. **28**, 3249 (1992).
[5] E. M. T. Velu, D. N. Lambeth, J. T. Thornton, and P.E. Russell, J. Appl. Phys. **75**, 6132 (1994).
[6] E. E. Fullerton, C. H. Sowers, J. Pearson, S. D. Bader, X. Z. Wu, and D. Lederman, Appl. Phys. Lett. **69**, 2438 (1996).
[7] E. E. Fullerton, J. S. Jiang, C. Rehm, C. H. Sowers, S. D. Bader, J. B. Patel, and X. Z. Wu, Appl. Phys. Lett. **71**, 1579 (1997).
[8] Yoshinohu Okumura, Osamu Suzuki, Hiroaki Morita, XingBo Yang, Hiroyasu Fujimori, J. Magn. Magn. Mater. **146**, 5 (1995).
[9] Y. Liu, B. W. Robertson, Z. S. Shan, S. H. Liou, and D. J. Sellmyer, J. Appl. Phys. **77**, 3837 (1995).
[10] Eric E. Fullerton, J. Samuel Jiang, C. H. Sowers, J. E. Pearson, and S. D. Bader, Appl. Phys. Lett. **72**, 380 (1998).
[11] J. P. Liu, Y. Liu, R. Skomski, and D. J. Sellmyer, J. Appl. Phys. **85**, 4812 (1999).
[12] R. Andreescu and M. J. OShea, International Journal of Modern Physics B **15**, 3243 (2001).
[13] Hansen, Binary Alloy Phase Diagrams, edited by Thaddeus B. Massalski, Published by Willian W. Scott, Jr. **805**, 2069 (1986).
[14] R. I. Mayo, K. O'Grady, P. E. Kelly, J. Cambridge, I. L. Sanders, T. Yogi, and R. W. Chantrell, J. Appl. Phys. **69**, 4733 (1991).
[15] C. Prados and G. C. Hadjipanayis, Appl. Phys. Lett. **74**, 430 (1999).
[16] Choong Jin Yang and CaiYin You, submitted to J. Appl. Phys. June (2002).